Biochimica et Biophysica Acta 1837 (2014) 825–834

Contents lists available at ScienceDirect

Biochimica et Biophysica Acta

journal homepage: www.elsevier.com/locate/bbabio

Redox and ATP control of photosynthetic cyclic electron flow in *Chlamydomonas reinhardtii* (II) Involvement of the PGR5–PGRL1 pathway under anaerobic conditions

Jean Alric *

UMR 7141, CNRS et Université Pierre et Marie Curie (Paris VI), Institut de Biologie Physico-Chimique, 13 rue Pierre et Marie Curie, 75005 Paris, France

ARTICLE INFO

Article history:
Received 8 October 2013
Received in revised form 29 January 2014
Accepted 30 January 2014
Available online 4 February 2014

Keywords:
Electron transfer
Green algae
Chlamydomonas reinhardtii
Photosystem I
Cytochrome b_6f

ABSTRACT

In oxygenic photosynthesis, cyclic electron flow around photosystem I denotes the recycling of electrons from stromal electron carriers (reduced nicotinamide adenine dinucleotide phosphate, NADPH, ferredoxin) towards the plastoquinone pool. Whether or not cyclic electron flow operates similarly in *Chlamydomonas* and plants has been a matter of debate. Here we would like to emphasize that despite the regulatory or metabolic differences that may exist between green algae and plants, the general mechanism of cyclic electron flow seems conserved across species. The most accurate way to describe cyclic electron flow remains to be a redox equilibration model, while the supramolecular reorganization of the thylakoid membrane (state transitions) has little impact on the maximal rate of cyclic electron flow. The maximum capacity of the cyclic pathways is shown to be around 60 electrons transferred per photosystem per second, which is in *Chlamydomonas* cells treated with 3(3,4-dichlorophenyl)-1,1-dimethylurea (DCMU) and placed under anoxic conditions. Part I of this work (aerobic conditions) was published in a previous issue of BBA-Bioenergetics (vol. 1797, pp. 44–51) (Alric et al., 2010).

1. Introduction

In addition to the linear transfer of electrons from the primary electron donor, water, to the terminal electron acceptor, $NADP^+$, involving both photosystems I and II, a cyclic electron transfer occurs around PSI. Cyclic electron flow participates in the building of a proton motive force across the thylakoid membrane because electron transfer is coupled to proton transfer at the level of the cytochrome b_6f complex. This proton gradient is used for ATP synthesis. Therefore, cyclic electron flow plays a role in increasing ATP at the expense of NADPH, providing a major regulatory control point in chloroplast metabolism. Not only did Arnon discover cyclic photophosphorylation, *i.e.* ATP synthesis induced by cyclic electron flow [2] but he also discussed the possible mechanisms of regulation of ATP and NADPH production in the balance between cyclic and non-cyclic (linear) photophosphorylation. He considered two models, a redox-equilibration model [3] where linear flow and cyclic flow are in competition with each other, and also a model where a fraction of PSI could be engaged specifically in cyclic electron flow.

By definition, cyclic electron flow is the recycling of electrons around PSI, *i.e.* it does not produce nor consume electrons. Upon a dark-to-light transition, the operation of cyclic electron flow in response to PSI excitation depends upon the reduction state of the electron carriers prior to illumination [4]. Following Bendall and Manasse [5], let us consider a simple model for cyclic electron flow where two extreme cases can be distinguished: (i) if the PQ and $NADP^+$ pools are fully oxidized, no electrons are available for recycling and cyclic electron flow will be null; (ii) the opposite instance is for fully reduced PQH_2 and NADPH pools, where in this case there is no electron acceptor available for PSI and cyclic electron flow is null again. Those two 'boundary conditions' were recently reached in plants (i) with a far red preillumination (sensitizing only PSI) [6], and (ii) with a broadband illumination (PSI + PSII) in the presence of iodoacetamide [7]. In between those two opposite cases, an optimal condition for the poise of redox carriers may exist where cyclic electron flow reaches its maximal rate. Crowther and Hind [8], Mills et al. [9], Slovacek et al. [10] and also Hosler and Yocum [11] have shown the importance of the redox poise of electron carriers for cyclic electron flow in isolated chloroplasts or thylakoid membranes reconstituted with ferredoxin, FNR and $NADP^+$/NADPH. In particular, they have shown a stimulating effect of DCMU in preventing over-reduction of the PQ pool. Allen proposes that the maximum cyclic rate is reached for a PQ pool half reduced [12]. The estimate of the proper redox poise required to reach the maximal cyclic electron flow rate depends on the enzymatic model considered, whether it is simply a redox equilibration, or if it involves activation steps, like activation by thioredoxins [13,14].

Abbreviations: PSII, photosystem II; PSI, photosystem I; P_{700}, primary electron donor of PSI (reduced form); P^+_{700}, primary electron donor of PSI (oxidized form); DCMU, 3(3,4-dichlorophenyl)-1,1-dimethylurea; HA, hydroxylamine

* Service de Biologie Végétale et de Microbiologie Environnementales, UMR 7265 (CNRS/CEA/Aix-Marseille Université) (SBVME), Laboratoire de Bioénergétique et Biotechnologie des Bactéries et Microalgues (LB3M), CEA Cadarache, 13108 Saint Paul Lez Durance, France.

E-mail address: jean.alric@cea.fr.

0005-2728/$ – see front matter © 2014 Elsevier B.V. All rights reserved.
http://dx.doi.org/10.1016/j.bbabio.2014.01.024

Lateral heterogeneity in PSI and PSII distribution in the thylakoid membranes [15,16] may also change the kinetic optimum. Cytochrome b_6f complex was found in both grana stacks and stroma lamellae [17,18] in a ratio that could be modulated by state transitions [19,20]. The role of state transitions in the possible regulation of cyclic electron flow has been studied in the green alga *Chlamydomonas reinhardtii* [21–27], and even very recently in the context of the isolation of a PSI-b_6f supercomplex [28,29]. Here these concepts are revisited using the *stt7–9* mutant, and similarly to that reported by Kramer and co-workers for plants [30] or *Chlamydomonas* [31], we conclude that cyclic electron flow is not simply governed by state transitions.

At variance with plants or other algae such as Chlorella, *C. reinhardtii* does not possess far-red absorbance bands for LHCI. It precludes the use of far red light as an excitation specific to PSI [1]. The use of DCMU circumvents this problem, blocking PSII photochemistry, but it does so in an irreversible manner: once poisoned with DCMU, PSII cannot be used to load the photosynthetic chain in electrons, as extensively used in plants by Joliot and Joliot [32]. Although this difference between *Chlamydomonas* and plants is not relevant to the mechanism of cyclic electron flow itself, it has to be taken into account because it represents a constraint at the experimental level. An alternative source for reductants is cellular metabolism in the dark. In *Chlamydomonas*, the dark reduction of the PQ pool is faster than in plants [33,34] and a model describing the redox poise of the PQ/PQH_2 and $NADP^+$/NADPH pools was previously proposed [4,35]. Instead of using PSII, this work uses chloroplast metabolism to load the photosynthetic electron transport chain in electrons prior to illumination.

In the first part of this work [1] we hypothesized that, in *Chlamydomonas*, the prevailing pathway under aerobic conditions, in the presence of DCMU was the one involving NAD(P)H-dehydrogenase (abbreviated NDH), likely corresponding to NDA2 [36]. Results herein show that it is indeed the case, consistent with a previous report on *pgrl1* [37] showing that the Proton Gradient Regulator 5–PGRL1 pathway (hereafter denoted PGR for short), or FQR for ferredoxin-quinone reductase [14,38], was clearly observed in samples poisoned with DCMU and placed under anaerobic conditions. From a functional point of view, the *pgr5* mutant [39] is virtually indistinguishable from *pgrl1* [37]. For the sake of simplicity, we shall here describe only *pgr5*.

Here we present a non-invasive method giving access to the maximal relative capacities of the NDH and PGR pathways *in vivo*. This contribution shall fulfill the request recently presented by Leister and Shikanai [40]: 'We currently lack a reliable way of measuring cyclic electron flow directly, and thus have no means of clearly distinguishing between partial and complete lack of cyclic electron flow'.

2. Materials and methods

2.1. Strains

C. reinhardtii WT and mutant strains were grown at 25 °C under photoheterotrophic conditions (Tris/Acetate/Phosphate (TAP) medium and light irradiance of $<10\ \mu E\cdot m^{-2}\cdot s^{-1}$). The mutant strain *pgr5* was obtained from Niyogi [39], *stt7–9* was obtained from Cardol [41], itself derived from *stt7* provided by Rochaix [42]. In exponential phase, cells were harvested by centrifugation at 4000 *g* for 5 min and resuspended in HEPES 20 mM pH 7.2 Ficoll 20% to a final concentration in PSI of about 50 nM (estimated from light-induced absorbance changes and $\Delta\varepsilon_{700\ nm} \sim -50\ mM^{-1}\cdot cm^{-1}$). Although resuspended in buffer, the cells were not washed free from acetate [33]. Inhibitors were purchased from Sigma. Unless stated otherwise, samples were systematically treated with 1 mM Hydroxylamine (HA) and 10 μM 3(3,4-dichlorophenyl)-1,1-dimethylurea (Diuron, or DCMU) to inhibit PSII (see below).

2.2. Optical spectroscopy

Absorbance changes at 705 and 520 nm were monitored using a JTS-10 (BioLogic) spectrophotometer as previously described in [1]. Saturating single turnover laser flashes were provided by a pulsed Nd:YAG laser (~6 ns duration, 532 nm) fitted to a broadband dye laser rod (~650 nm, from Continuum Biomedical ConBio Multilite Dye Laser). Cells were poisoned with 10 μM DCMU and 1 mM HA. These inhibitors serve two purposes. First, in *Chlamydomonas*, due to the absence of PSI far-red absorbance bands, it is necessary to block PSII to accumulate P_{700}^+ under continuous illumination [1]. Second, under such conditions, when Q_B of PSII is blocked by DCMU, and after a preillumination (*i.e.* a first charge separation P_{680}^+–Q_A^-), P_{680}^+ is reduced by HA, and PSII irreversibly blocked in the P_{680}–Q_A^- state, which corresponds to the maximum yield of chlorophyll fluorescence, F_M or F_M'. This F_M' value is used to follow state transitions (see below).

Actinic light was provided by a green LED (~530 nm, ~300 μE $\cdot m^{-2}\cdot s^{-1}$) which was turned on for 10 μs, 1 s or 20 min. P_{700}^+ was accumulated following 1 s of illumination, similarly as described in [1], see Fig. 1A for example (light is on between the upward and downward arrows). Hereafter we also refer to this fraction as photo-oxidizable P_{700}. F_M' was probed by a repetition of 4 pulses of 10 μs duration (see horizontal arrow in Fig. 1A). Here detected as an absorbance change, the chlorophyll fluorescence yield appears negative, see -F_M' label in Fig. 1A or B. The 20 min light period represented as a white bar in Fig. 2 (see also upward and downward arrows) was interrupted for 6 s during which absorbance and fluorescence were measured (see Fig. 1D or E for example) identically as in Fig. 1A. Probed only 3 s apart, P_{700}^+ and F_M' can be considered as sampled almost simultaneously when compared to the time-frame of the slow anaerobic adaptation kinetics, reported in Fig. 2.

2.3. Monitoring of state transitions

Here *Chlamydomonas* cells were grown in low light. Under such conditions they do not accumulate LHCSR3 (the algal counterpart of PsbS) and, as a consequence, they do not show any qE component of NPQ [43]. In the absence of any strong and prolonged illumination ($>500\ \mu E\cdot m^{-2}\cdot s^{-1}$, >30 min) that would induce photoinhibition (qI), fluorescence quenching is therefore attributable unambiguously to state transitions (qT). Such a strong correlation between State 1 and high F_M' level or State 2 and low F_M' level has been extensively shown using 77 K fluorescence spectra and phosphorylation patterns of thylakoid membrane proteins [44,45]. Here we used F_M' to monitor the kinetics of state transitions (Fig. 2) and verified our attribution to State 1 or State 2 with 77 K emission spectra (not shown).

2.4. Monitoring of oxygen tension

Aerobic conditions were achieved after a vigorous stirring of the sample in air. Anaerobic conditions were reached after typically 20 min adaptation in sealed cuvettes owing to mitochondrial respiration of the cells. While monitoring absorbance at 705 nm, oxygen tension was measured with a Clark microelectrode (MLT1120, ADInstruments) in a glass cuvette designed for redox titrations. Absorbance and oxygen measurements were done 30 s apart. The measurement of absorbance changes in whole cells, which required a high sensitivity of optical detection (the total amount of P_{700}^+ was less than 10^{-2} O.D.), was incompatible with the continuous stirring of such a turbid sample. On the contrary, proper oxygen measurements require a vigorous agitation for a rapid equilibration of oxygen between the sample and the Clark electrode (which itself consumes oxygen).

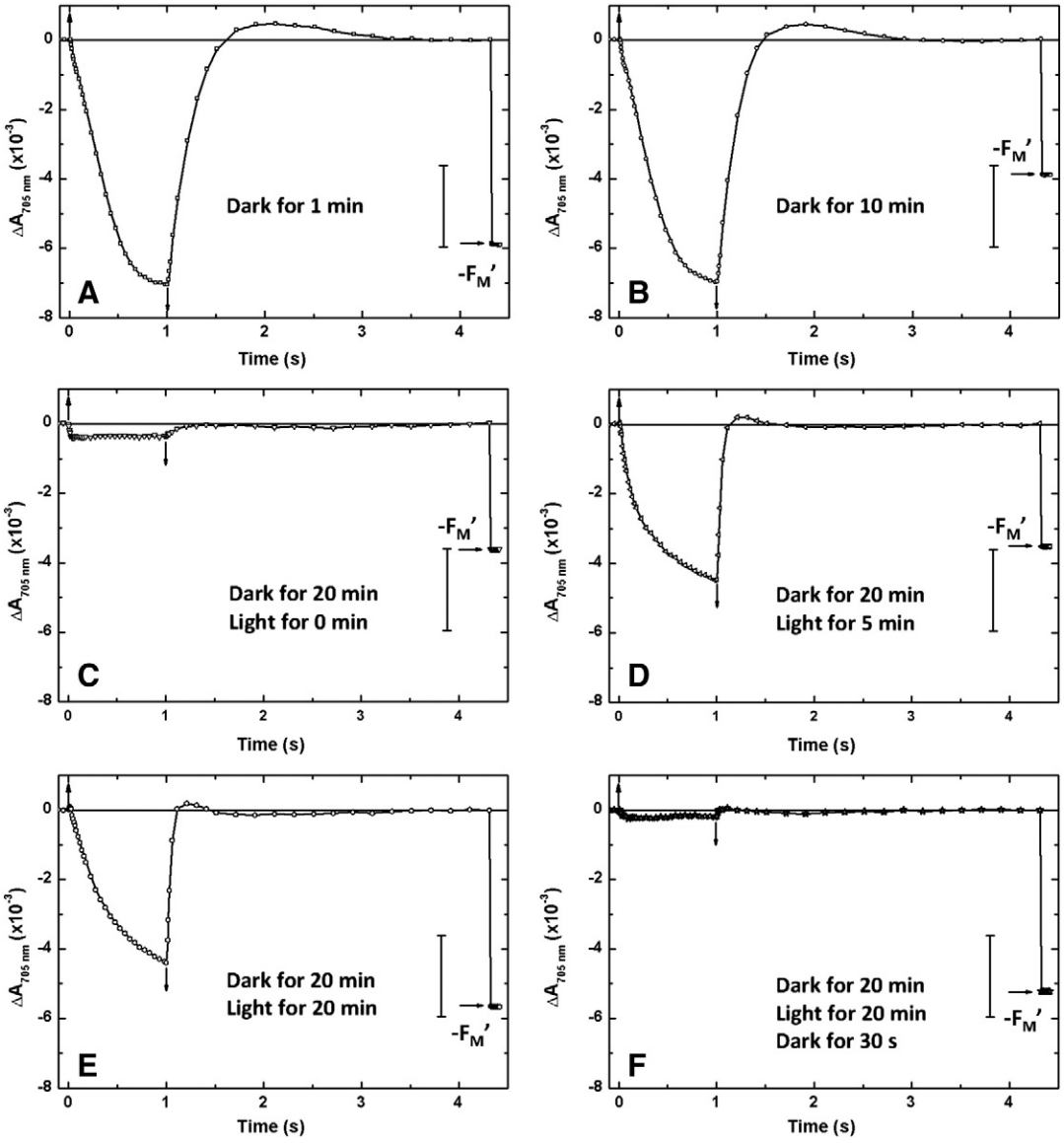

Fig. 1. Simultaneous monitoring of P_{700} oxidizability (left axis, absorbance changes at 705 nm) and state transitions (see bar scale on the right, next to the maximum yield of fluorescence F_M'). Intact cells of *Chlamydomonas reinhardtii* devoid of PSII activity (treated with DCMU and hydroxylamine) were adapted under anaerobic conditions during an hour. The measurement sequence is identical in the six panels, and composed of a baseline in the dark ($t < 0$) for 2 s (not shown), a continuous illumination from $t = 0$ to 1 s to probe P_{700} oxidizability (see upward and downward arrows), a dark period of 3 s during which P_{700} is re-reduced, and 4 pulses of 10 μs duration to probe F_M'. The incubation period was divided into three phases of 20 min duration, in the dark (A, B, C), in the light (D, E) and in the dark again (F). The light used in the second phase was interrupted for 6 s during the measurement. The amplitudes of the F_M' and P_{700}^+ signals are reported in Fig. 2 as a function of the incubation time.

2.5. Kinetic analysis after cessation of illumination

Here we know no better than to refer to the appendix by Kuntz and Calvin [46], where some of the principles of the kinetic analysis of flow rates in photosynthesis are elegantly described and reproduced hereafter. Looking at any intermediate in the photosynthetic chain (for instance P_{700}^+ or cyt f^+), at steady-state in the light the production rate of an intermediate is equal to the destruction rate of this intermediate. For those intermediates directly involved in a photochemical reaction, the cessation of illumination will instantly drop the production rate to zero. Thus, after a steady-state is reached in the light, a measure of the initial rate of the destruction reaction upon light-to-dark transition will tell us exactly what the production rate was in the light. That the reaction intermediate considered in the kinetic analysis has to be directly linked to a photochemical reaction is crucial. P_{700} will do, as well as the membrane potential P_{515} or electrochromic shift (ECS), both used in this study, but not cyt *f*. Cyt *f* dark reduction shows a lag, being delayed by the transfer of electrons to a small pool of downstream electron acceptors: oxidized plastocyanin and P_{700}^+, also accumulated in the light.

Although we expect to observe a rather exponential reduction of P_{700} we do not expect the decay of the membrane potential to be monophasic: we will base our analysis on the first tens of milliseconds after cessation of illumination. For more details on the analysis of P_{515} decay, see the extensive work of Kramer and co-workers [47–51].

Unless stated otherwise, in this study PSII is inactivated by HA and DCMU, therefore only PSI contributes to photochemistry and to the building of the membrane potential. Lucker and Kramer have shown (and we have observed the same) that under such conditions, cyclic electron flow measured as P_{700} reduction or P_{515} decay yield identical rates [31].

As proposed by Joliot and Joliot [50], normalizing ECS on one charge transferred across the membrane per PSI (signal induced by a saturating single turnover flash) provides us with a direct way of expressing the flow of electrons (or protons) through the membrane, *i.e.* directly

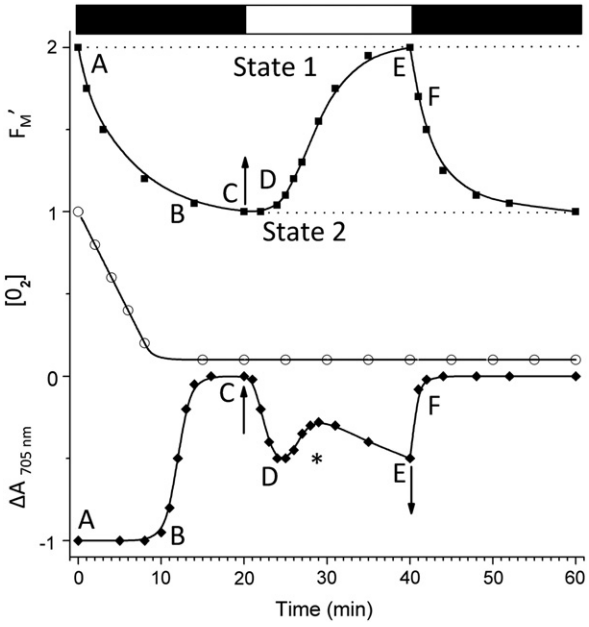

Fig. 2. Simultaneous monitoring of state transitions (top), oxygen tension (middle) and P_{700} photooxidation (bottom) upon anaerobic incubation of intact cells of *Chlamydomonas reinhardtii* devoid of PSII activity (treated with DCMU and hydroxylamine). Data were normalized. Upward arrows denote the time when a continuous illumination was turned on between measurements, and downward arrows show when it was turned off (see also horizontal white and black bars). Capital letters are used in the text for commenting the data and correspond to the different panels of Fig. 1.

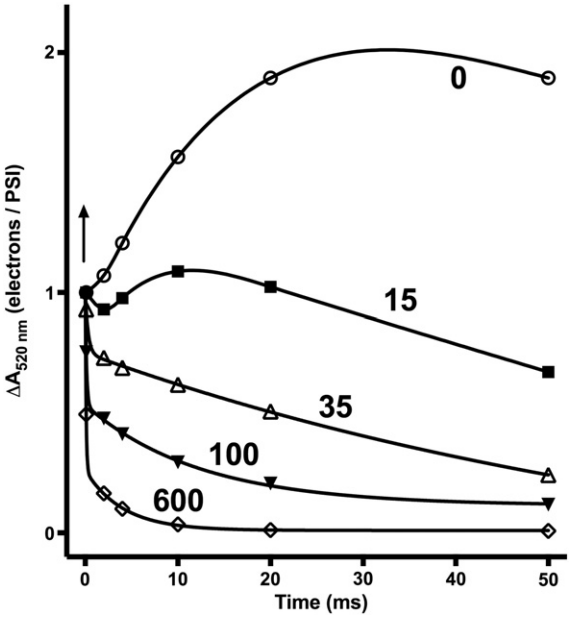

Fig. 3. Changes in membrane potential induced by a single turnover (6 ns) saturating flash, monitored as an electrochromic shift of carotenoids at 520 nm. *Chlamydomonas* cells were treated with DCMU and hydroxylamine and adapted anaerobically for 20 min. Curve 0 corresponds to the dark-adapted sample, while the other curves were obtained with a background continuous illumination giving an initial photochemical rate of 15, 35, 100 or 600 electrons transferred per second per PSI. The two top curves were interpolated, the three bottom data were fitted to a bi-exponential decay constrained to 1 at $t = 0$. The first data point was taken 150 μs after the flash. At 600 $e^- \cdot s^{-1}$, see open diamonds, the first data point being at amplitude ~ 0.5 shows a very fast reduction phase of $t_{1/2} < 150$ μs.

proportional to ν_{H+} in Kramer's nomenclature, see [52]. Klughammer et al. proposed recently an accessory for their Dual-PAM-100 aiming at getting the same information [53], although with an indirect determination of PSI contribution (without a proper single turnover saturating flash). Here the flow rates are expressed in $e^- \cdot s^{-1}$ per PSI. This method, used below to assess cyclic electron flow rates, also serves to calibrate the intensities of the continuous light. Upon a dark-to-light transition, the rise-time of the ECS signal gives the initial photochemical rate of PSI, or the actinic effect of light. Here 15, 35, 100 or 600 $e^- \cdot s^{-1}$ was transferred initially per PSI (not shown, but the corresponding rates are reported on Fig. 3 where such actinic lights were used, provided by a red LED at ~630 nm).

2.6. Conversion between photosynthetic rates and metabolic fluxes

Under steady-state, in a heterogeneous system, a distribution of flow rates may be found. In other words, the number of electrons flowing through a given photosystem per unit time may not be the same as for another photosystem. In this work, when linear or cyclic electron flow rates are considered, "average" flow rates are meant, *i.e.* relative to the total amount of photosystems. If k is the average photochemical rate (in s^{-1}) and [Q] the relative quantity of active, or "open" photosystems (in number of electrons that can be transferred per total amount of photosystems), the average flow rate is $F = k\,[Q]$ (in $e^- \cdot s^{-1} \cdot PS^{-1}$).

A single turnover saturating flash is used for normalization to obtain the total amount of PSI in samples treated with HA and DCMU (inhibited for PSII). For the comparison of our data, directly expressed in electrons transferred per second per photosystem I ($e^- \cdot s^{-1} \cdot PSI^{-1}$), with other metabolic studies where rates are usually expressed in $\mu mol_{metabolite} \cdot h^{-1} \cdot mg_{Chl}^{-1}$, we have estimated, from absorbance changes at 700 nm, that for a concentration in PSI of about 50 nM ($\Delta\varepsilon_{700\ nm} \sim -50\ mM^{-1} \cdot cm^{-1}$), the chlorophyll content was typically 45 $\mu g_{Chl} \cdot ml^{-1}$ [54]. Given that 1 mg_{Chl} is approximately equal to 1.1 μmol_{Chl}, 45 $\mu g_{Chl} \cdot ml^{-1}$ corresponds to 49.5 μM_{Chl}, *i.e.* about 1000 times more than PSI, consistent with other reports [55]. It provides us with the ruler: 1 $e^- \cdot s^{-1} \cdot PSI^{-1} \approx 4\ \mu mol_{e^-} \cdot h^{-1} \cdot mg_{Chl}^{-1} =$ 1 $\mu mol\ O_2 \cdot h^{-1} \cdot mg_{Chl}^{-1}$ [33]. Under such growth conditions, PSII is in stoichiometric amounts with PSI, making the electron flow rate identical for PSII and PSI.

3. Results

3.1. Redox changes upon anaerobic adaptation

Figs. 1 and 2 show the results of a typical experiment of simultaneous sampling of different parameters upon anaerobic adaptation of a suspension of *C. reinhardtii* cells, treated with HA and DCMU, first in the dark for 20 min, and then in the light for 20 more minutes, with a relaxation in the dark for 20 min (see black and white bars in Fig. 2) so that the whole experiment lasted for an hour. The various panels in Fig. 1 show light-induced absorbance and fluorescence changes at discrete time points, labeled from A to F, and the same letters are reported in Fig. 2 in order to spot when the experiments of Fig. 1 were done. A vertical bar scale next to F_M' is reported identically for each panel in Fig. 1. It represents the maximum amplitude of the changes in F_M' throughout the whole experiment. Under such conditions, F_M' reflects state transitions (verified by 77 K fluorescence emission spectra at A, C and E time-points, not shown), see Materials and methods section for more details. During this experiment, no oxygen is evolved due to the inhibition of PSII by HA and DCMU.

Upon anaerobic adaptation, the concentration of oxygen steadily decreases in the sample, see A–B time-points in Fig. 2, and also F_M' decreases, showing a state transition from state 1 to state 2. Meanwhile the photo-oxidizable fraction of P_{700} remains very stable, in terms of amplitude and also re-reduction rate (compare Fig. 1A and B). At around 13 min (see B–C transition in Fig. 2), the amount of photo-oxidizable P_{700} decreases sharply to less than 10% of the initial value (compare Fig. 1B and Fig. 1C). This delay for reaching anoxia, here of 13 min, will depend on the respiration rate, itself dependent on the concentration of the cells, as well as the presence or absence of acetate, but a sharp

decay in P_{700} oxidizability will always be obtained. Such an abrupt decline coincides with the depletion of oxygen in the sample, and it is attributed to limitations at the acceptor side of PSI in anoxia. Upon depletion of oxygen in the sample, the back-up of reductants from the mitochondrion to the chloroplast was estimated as less than 30 s, the minimal delay between an absorbance measurement and an oxygen measurement (see the experimental limitations detailed in the Materials and methods section). After a stable anaerobic state is reached (C), a continuous illumination is turned on (300 $\mu E \cdot m^{-2} \cdot s^{-1}$), which lasted for 20 min. Such continuous background illumination was only turned off for short intervals of 6 s, to allow the sampling of P_{700} and F_M', identically as in Fig. 1A. Similarly to that reported by Delepelaire and Wollman [44] who used a very similar protocol, we observed a lag in the rise of F_M' in the light (see Fig. 2). The duration of this lag increases with the time of adaptation in the dark (not shown here but in [44]). Here we show that the fraction of photo-oxidizable P_{700} shows also a lag, although briefer. The amplitude of photo-oxidizable P_{700} during the D–E transition shows an overshoot, marked by an asterisk in Fig. 2. It was a reproducible phenomenon that we attributed partly to a change in PSI antenna size. It was because this overshoot coincided with the rise of F_M' (transition to state 1). The kinetics of P_{700} oxidation were expectedly faster in Fig. 1D (larger PSI antenna size in state 2) than in Fig. 1E. It is not clear, however, why the amplitude of P_{700}^{+} is not larger in D than in E as it would be expected from a simple kinetic model. It may have to do with a change in the pool size of PSI electron acceptors between D and E time points, as further discussed below.

Anoxic P_{700} oxidizability was blocked almost instantly after 30 s of dark adaptation while F_M' barely changed (compare E and F time points in Fig. 1 and 2). It shows again the tight coupling between light reactions and chloroplast metabolism and the quick back-up of electrons onto the photosynthetic electron transfer chain in anoxic conditions.

When comparing the F_M' value and the P_{700} reduction rate in panels A, B, D and E from Fig. 1 it is obvious that there is no strict correlation between state transitions and P_{700} reduction rate: P_{700} reduction being equally slow (~10 s^{-1}) in state 1 (panel A) or state 2 (panel B) or being similarly fast (~40 s^{-1}) in state 2 (panel D) or in state 1 (panel E). These findings that show a lack of a strict correlation between state transitions and P_{700} reduction rates are very similar to that reported in [28].

3.2. Fraction of photochemically active PSI centers

In Fig. 3 are shown the electrogenic events through the thylakoid membrane (P_{515} or ECS for electrochromic shift of carotenoids), induced by a very short and intense flash (~6 ns, see upward arrow), saturating for PSI and giving a single photochemical turnover (only one electron transferred per PSI during the flash). A continuous red light, provided by a LED (~630 nm) is used to provide a continuous background illumination. Fig. 3 shows the response of ECS induced by the flash only, the effect of the continuous illumination being subtracted to draw the baseline. The labels on the curves refer to the light intensities expressed as initial photochemical rates of PSI in $e^- \cdot s^{-1}$. Here again, intact cells were poisoned with HA and DCMU so that PSII is totally inhibited (see Materials and methods) and does not contribute to the membrane potential, detected at 520 nm, at $t \geq 150$ μs. Anaerobic conditions were achieved similarly as described above in Figs. 1 or 2 (see data point C).

In the dark (see open circles in Fig. 3), and similarly to that reported previously [56], after an instantaneous rise of absorbance induced by the flash (see upward arrow), a slow rise of nearly 10 ms half-time is observed. The instantaneous phase corresponds to one charge separation in PSI, hence the normalization to 1 on the first data point at $t =$ 150 μs. The same normalization factor was applied to the other curves obtained in the presence of a background illumination. The ~10 ms phase corresponds to electron transfer in the cyt b_6f complex [56]. Whereas this slow electrogenic phase is still observed in the presence of a weak continuous light (see closed squares, 15 $e^- \cdot s^{-1}$), it disappears at higher light intensities. Instead, in the presence of a stronger continuous illumination, a very fast decay develops that makes the instantaneous phase appear even smaller: the first data point at $t =$ 150 μs reaches only half of the initial amplitude under strong illumination (600 $e^- \cdot s^{-1}$ per PSI, see open diamonds). Such a fast destruction of the membrane potential under light anaerobic conditions is very likely due to charge recombination in PSI, as further discussed below.

3.3. Sustained cyclic electron flow in anoxia in the presence of DCMU and hydroxylamine

In Fig. 4, a dark adapted sample was preilluminated for 3 s with saturating light (600 $e^- \cdot s^{-1}$), inducing an accumulation of membrane potential and giving an increase in absorbance (ECS) at 520 nm (not shown). After 1–3 s of illumination, ECS reached a steady-state level, meaning that the building of membrane potential by photochemical reactions was exactly compensated by the destruction of the membrane potential. A baseline was drawn at steady state during illumination ($t < 0$). At $t = 0$, instead of giving a flash like in Fig. 3, the continuous light was turned off (see downward arrow), instantly stopping the activity of the photosystems. The membrane potential decayed in the dark, as shown in Fig. 4. Because the system was at steady state in the light, the post-illumination decay rate is exactly equal to what the photochemical rate was in the light. In order to provide the most accurate comparison between WT and mutant strains, we normalized the amplitude of the ECS on the flash-induced signal obtained in dark-adapted conditions and corresponding to one charge transferred across the membrane per PSI center [50] (cells were treated with DCMU and hydroxylamine, see open circles in Fig. 3 for the WT, not shown for the mutants). After this normalization on PSI we measured directly electron flow rates, proportional to the v_{H+} term in Kramer's nomenclature [52]. In Fig. 4, right panels (A′, B′ and C′) are zooms of left panels (A, B and C). In panel A, a dotted rectangle materializes the zooming area. In the six different panels in Fig. 4, for the ease of comparison, the data obtained for WT cells poisoned with DCMU and placed under either oxic (ox) or anoxic (anox) conditions (circles) are reported. In panels A and A′, the comparison is against untreated cells (squares), in panels B and B′ the WT is compared to the *pgr5* mutant [39] (triangles), and in panels C and C′ the *stt7–9* mutant [41,42] (diamonds). In Table 1 various electron transfer rates are shown, from this work (average and error-bars obtained from at least three biological replicates) and from other studies in *C. reinhardtii*.

Here a graphical evaluation of the flow rates, illustrated in Fig. 4A′ and B′ is also shown. The slopes of the tangent arrows in panels A′ and B′ give the initial decay rates. Fig. 4A and A′ shows that the fastest electron flow is obtained for untreated WT aerobic cells (open squares). ECS decayed of 2 charges in nearly 10 ms (see arrow and dotted lines in panel A′) *i.e.* corresponding to $\tau \approx 5$ ms for 1 electron transferred through PSI, giving about $k = 1/\tau \approx 200\ s^{-1}$, *i.e.* a flow rate of 200 $e^- \cdot s^{-1} \cdot PSI^{-1}$ for the overall photosynthetic electron flow (linear + cyclic). When DCMU is added (open circles), the decay of the 520 nm signal is much slower (a tangent line interpolates an amplitude of −1 at ~70 ms, giving about 14 $e^- \cdot s^{-1}$) and exactly matched P_{700} reduction rate (not shown here, but see [1,31,33]). This rate reflects cyclic electron flow around PSI [1]. Under anoxic conditions (solid symbols), cyclic electron transfer rate was significantly accelerated (closed circles). ECS decayed one charge with a time constant of $\tau \approx 15$ ms (see B′), *i.e.* $k = 1/\tau \approx 66\ s^{-1}$.

An acceleration of cyclic electron flow was therefore observed in the presence of DCMU and induced by anoxic conditions. Whether this stimulation was due to state transitions or to other mechanisms was tested in experiments shown in the bottom four panels of Fig. 4.

Contrary to that hypothesized by Finazzi and coworkers [21–27], but supporting more recent work from Rappaport and co-workers [28] and Lucker and Kramer [31], such 'activation' of cyclic electron flow under

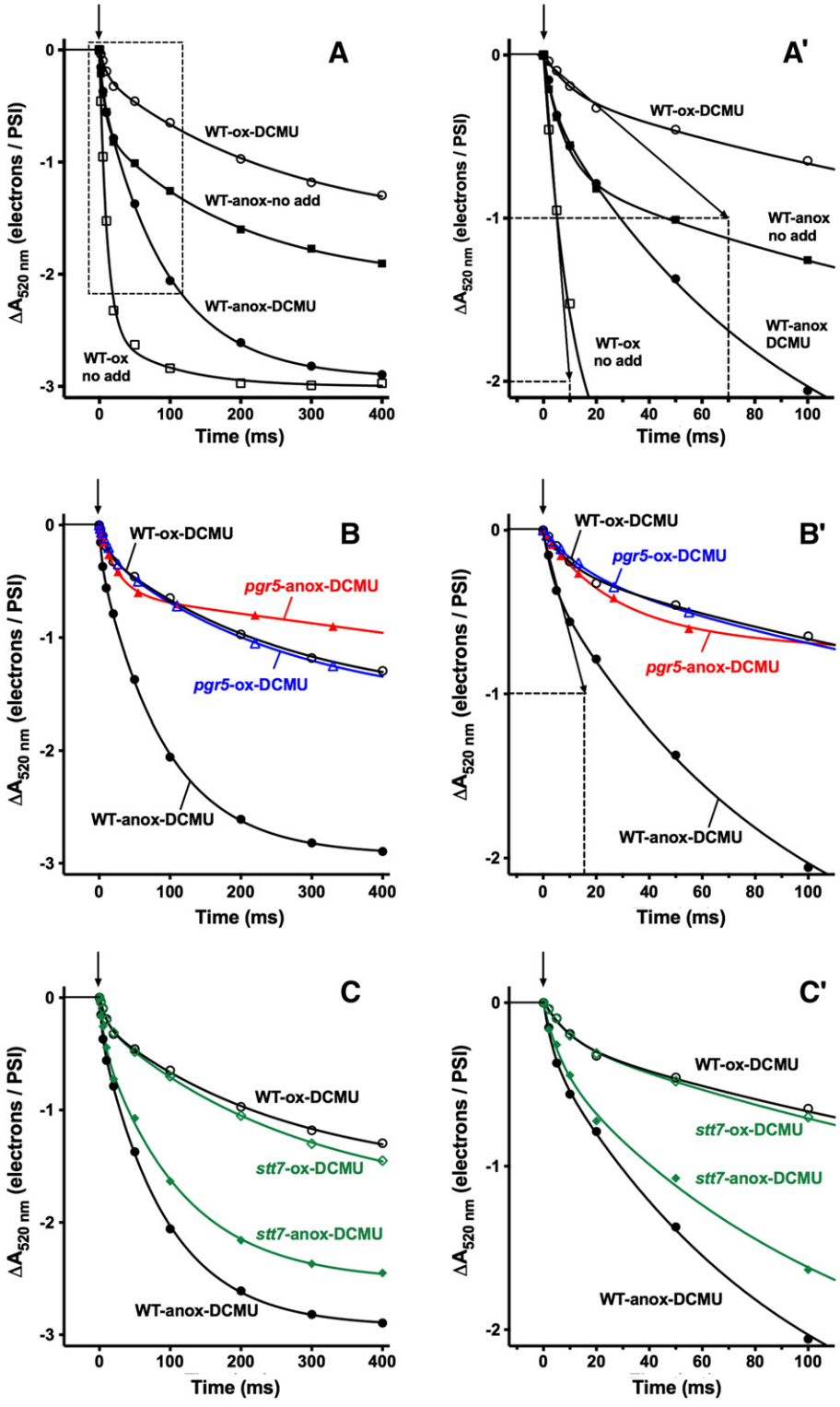

Fig. 4. Decay of the membrane potential upon a light-to-dark transition. For the calibration of the ordinates, the flash-induced absorbance change was measured for each different strain similarly as in Fig. 3 (open circles), so as to normalize the amplitudes obtained in different strains to 1 electron transferred per PSI. After 3 s of illumination, the membrane potential reached a steady-state level (not shown) here shifted to zero for a better comparison of the decay rates. The downward arrow shows when illumination was turned off. *Chlamydomonas* cells were placed under different conditions oxic (ox) or anoxic (anox) in the presence or absence of DCMU. For the ease of comparison, the data obtained for the WT, treated with DCMU, are reported identically in all six panels. The kinetics shown here are the result of a single representative experiment. For experimental variations (error bars), please refer to Table 1. The *pgr5* strain (B, B′) was obtained from [39], and the *stt7–9* strain (C, C′) from [41].

anaerobic conditions in the presence of DCMU is not due to state transitions because it is also observed in *stt7–9*, locked in state 1 (see panels C and C′). It is more likely attributable to the PGR pathway, as already shown for PGRL1 [37] and confirmed here for PGR5 (panels B and B′). In our hands, and in the experimental conditions used in Fig. 4, *pgr5* and *pgrl1* mutants are virtually indistinguishable. See also Table 1 for a compilation of the cyclic electron flow rates obtained in different conditions and different *Chlamydomonas* strains.

Table 1
Summary of the data obtained on cyclic electron flow rates and comparison with other data from the literature, treated with DCMU.

	Aerobic	Anaerobic	Reference
WT	**10 ± 3**	**60 ± 10**	**This work**
	15 ± 3	40 ± 5	[28]
	36 ± 2	46 ± 4	[37]
pgr5	**11 ± 5**	**16 ± 6**	**This work**
pgrl1	23 ± 2	23 ± 2	[37]
stt7	**10 ± 2**	**49 ± 9**	**This work**
	17 ± 3	33 ± 5	[28]

4. Discussion

In *Chlamydomonas* cells treated with DCMU and placed under anaerobic conditions, the oxidized form of the primary electron donor of photosystem I, P_{700}^{+}, cannot be accumulated under continuous illumination [4]; this is similar to that reported for the cyanobacterium *Arthrospira platensis* [57]. *Chlamydomonas* P_{700} oxidizability has been studied in two recent articles [28,58]. The state corresponding here to data point C in Fig. 1 or 2 is stable for 10–20 min. P_{700} can be partly photo-oxidized again after >20 min of anoxia, either because of the reoxidation of NAD(P)H in the dark by fermentative metabolism [28], or because of the synthesis of hydrogenase, an alternative electron acceptor for PSI [58]. Here we show that a similar PSI activity can be restored, prior to the activation of fermentative metabolism, if in between the measurements is inserted a continuous green illumination (530 nm, 300 $\mu E \cdot m^{-2} \cdot s^{-1}$), see data points D–E. The presence of DCMU in our samples blocks oxygen production in the light and rules out any direct or indirect effect of oxygen in the re-oxidation of P_{700} in the light. Fig. 2 shows an increase of F_M' in the light, revealing a transition from state 2 to state 1, as previously reported [44]. Such state 2 to state 1 transition was shown to be dependent upon cyclic photophosphorylation [59]. Here we show a direct link between the formation of state 1 and the oxidation of chloroplast electron carriers in the light, P_{700} and expectedly the PQ pool. Anoxic P_{700} photo-oxidation did not occur in FUD50, a mutant devoid of ATPase (not shown), while P_{700} photo-oxidation was still observed in a mutant devoid of Rubisco (not shown) suggesting that, in addition to the Calvin cycle, other ATP-requiring reactions are involved in chloroplast metabolic pathways oxidizing NADPH or ferredoxin to regenerate electron acceptors for PSI.

In this work, an experimental protocol is described that allows the measure of cyclic electron flow rates around PSI, see Fig. 4. Such a method has been largely developed and used in the last years by the group of Kramer [47–49,51] and sometimes denoted as DIRK (dark interval recovery kinetics or ECS for electrochromic shift). A recent and useful addition from Joliot and Joliot [50] was to express the flow rates in terms of electrons transferred per second per photosystem I. Here we used this normalization. As detailed in the Materials and methods section and firstly reported in [33], in *Chlamydomonas* cells grown in acetate containing medium under low light, an estimate can be made from the concentration in chlorophyll and PSI that 1 $e^- \cdot s^{-1} \cdot PSI^{-1} \approx$ 1 µmol $O_2 \cdot h^{-1} \cdot mg_{Chl}^{-1}$, therefore providing an easy conversion between our work and other studies. This estimate is verified independently by comparing these values of electron transfer rate in the absence of DCMU, 150–200 $e^- \cdot s^{-1} \cdot PSI^{-1}$ (Fig. 4A and A′ open squares), to the values reported for oxygen evolution from PSII (from gas exchange measurements) ranging between 120 µmol $O_2 \cdot h^{-1} \cdot mg_{Chl}^{-1}$ [60] and 200 µmol $O_2 \cdot h^{-1} \cdot mg_{Chl}^{-1}$ [61].

In the presence of DCMU (inactive PSII), any sustained electron flow is surely attributable to cyclic electron flow around PSI. In part I of our study, devoted to aerobic conditions [1], we reported rather slow rates of cyclic electron flow (<15 $e^- \cdot s^{-1} \cdot PSI^{-1}$), although we suggested that in the absence of DCMU, when PSII provides a reducing pressure on the electron transfer chain, participating in the production of NADPH, the flow rate of cyclic was expected to increase. In a subsequent study, we then analyzed how the dark chloroplast metabolism modulates the rates of cyclic under aerobic conditions [33], finding rates increasing up to 30 $e^- \cdot s^{-1} \cdot PSI^{-1}$ in a starchless mutant fed with acetate. Here it is shown that the cyclic rate is further increased under PSII inhibited anoxic conditions (~60 $e^- \cdot s^{-1} \cdot PSI^{-1}$), as already reported in [37] and more recently in [28]. We show that such an increase in cyclic rate is attributable to the PGR pathway, supporting some previous work [37], and is independent from state transitions, supporting that reported in [28,30,31], and further disproving previous opinions [21–27].

4.1. Charge recombinations in PSI under anaerobic conditions

P_{700} reduction rate (and also P_{700}^{+} steady-state level in the light) is a function of forward and reverse electron transfer, *i.e.* in the presence of DCMU, cyclic electron flow and charge recombination with PSI electron acceptors. Upon anaerobic adaptation, although an increase in cyclic electron flow is expected (more NADPH or reduced ferredoxin to serve as a substrate to the NDH or PGR pathways), we also expect an increase in charge recombination (increasing the concentration of reduced ferredoxin translates into a reduction of PSI electron acceptors F_A/F_B). P_{700}^{+} is not accumulated in the light under anaerobic conditions. It shows that P_{700} reduction rate is faster than its oxidation rate. It is, under light limiting conditions, because cyclic electron flow is faster than the actinic effect of light. Under 'saturating light' conditions we would expect to accumulate P_{700}^{+} if electron transfer was not limited at the acceptor side of PSI. 'Saturating light' conditions refer to a light intensity that largely exceeds the photosynthetic capacity of about 150–200 $e^- \cdot s^{-1}$ [62]. The highest light intensity used in this work, giving initial photochemical rates of 600 $e^- \cdot s^{-1}$, can be defined as such. Under anaerobic conditions P_{700}^{+} cannot be accumulated, even under such strong illumination (not shown). This observation suggests the occurrence of acceptor side limitations.

When considering a simple first order reaction, the flow of P_{700} oxidation is k_{ox} $[P_{700}]$, the flow of reduction being k_{red} $[P_{700}^{+}]$. At steady-state, the reduction flow rate being equal to the oxidation flow rate, and substituting $[P_{700}] = 1 - [P_{700}^{+}]$, one obtains $[P_{700}^{+}] = k_{ox}/(k_{ox} + k_{red})$. The oxidation rate k_{ox} is only dependent on the light intensity and it can be easily measured as the initial photochemical rate when all PSI centers are active (here 600 s^{-1}). The reduction rate k_{red} depends upon the reaction that is considered. For charge recombination in PSI, typical recombination times range between $t_{1/2} < 250$ µs (*i.e.* $k_{red} > 2700\ s^{-1}$) for P_{700}^{+}–A_1^{-}, $t_{1/2} = 1$ ms (k_{red} ~ 700 s^{-1}) for P_{700}^{+}–F_X^{-}, $t_{1/2} = 10$ ms (k_{red} ~ 70 s^{-1}) for P_{700}^{+}–$(F_AF_B)^{2-}$ and $t_{1/2} = 80$ ms (k_{red} ~ 8.7 s^{-1}) for P_{700}^{+}–$(F_AF_B)^{-}$ [63]. As shown in Fig. 3, a recombination event occurs within less than 250 µs after a flash, likely corresponding to the P_{700}^{+}–A_1^{-} recombination (see above). It suggests that P_{700}–F_X^{-} would be steadily populated under the continuous background illumination. The recombination rate of this charge-separated state (700 s^{-1}) is expectedly in the same order as the actinic effect of light on PSI (600 s^{-1}) narrowing our estimate to a half populated P_{700}–F_X^{-} state (46% = 600/(600 + 700)).

To summarize our investigations about limitations at the acceptor side of PSI in anoxia, and to make it sound for the interpretation of cyclic electron flow, we can formulate a simple conclusion: in anoxic conditions, PSI acceptor-side limitations rule out any relevant analysis of cyclic flow based on the amounts (oxidized/total) of carriers accumulated in the light, whether it is P_{700} or cyt *f*, which equilibrates with P_{700} and therefore reflects PSI limitation as well [21–27].

However, the absence of P_{700}^{+} accumulated in the light ensures that post-illumination kinetics of the membrane potential (Fig. 4) reflect productive electron flow and not charge recombination. In other words, PSI cannot recombine because there is no P_{700}^{+} to recombine with. In the presence of DCMU, any sustained electron flow

under anoxia is therefore attributable unambiguously to cyclic electron flow.

Apart from drawing our attention towards electron transfer limitation at the acceptor side of PSI, the experiments described in this section also show that ferredoxin must be fully reduced in light-anaerobic conditions, a situation favorable to the monitoring of PGR mediated cyclic electron flow (see below).

4.2. Redox poise of the chloroplast in the light

Under aerobic conditions, P_{700}^{+} is accumulated in the light whereas it is not under anaerobic conditions. It means that under oxic conditions and prior to illumination, the pool size of oxidized PSI electrons acceptors ($NADP^{+}$, oxidized ferredoxin and FNR) is greater than the pool size of reduced PSI secondary electron donors (plastocyanin, cytochrome *f*, Rieske, plus a few plastoquinols). In anoxia it is the reverse situation: the pool size of pre-oxidized acceptors is smaller than the pool size of pre-reduced donors. It shows that the total pools of PQ/PQH_2 and $NADP^{+}$/NADPH must be of similar sizes [4]. We have made an observation on the side that allows narrowing this estimate. In a *Chlamydomonas* mutant devoid of cytochrome b_6f complex, and adapted to anaerobic conditions, the amplitude of P_{700}^{+} accumulated under continuous illumination is only ~90% of the one reached under aerobic conditions (not shown). In this instance, the number of PSI secondary electron donors is restricted to ~2 electrons present on plastocyanin in the dark (no cytochrome b_6f complex). It suggests that for a given PSI center only ferredoxin and FNR can accept these only ~2 electrons. This experiment provides compelling evidence of the very reductive poise of the stroma under anaerobic conditions and the limitation that bears at the acceptor side of PSI: $NADP^{+}$ availability becomes limiting for accepting electrons from P_{700}. The redox poise of the stroma under dark anaerobic conditions is therefore likely to be in the range of $E_h \approx -380$ mV, *i.e.* somehow ~60 mV below the E_m of $NADP^{+}$/NADPH of −320 mV to ensure a significant reduction of the NADPH pool.

4.3. The maximum cyclic electron flow rate is likely around 60 $e^{-}\cdot s^{-1}\cdot PSI^{-1}$

Here the emphasis is that the electron flow rate reported in this work for anaerobic, DCMU treated cells is very likely the maximum rate for cyclic electron flow.

As thoroughly discussed in [4], and also briefly reported in the Introduction, the optimal conditions to observe cyclic electron flow are not easily reached *in vivo*. If linear electron flow is active, NADPH and reduced ferredoxin are accumulated, but the PQ pool also becomes reduced, therefore decreasing the concentration of electron acceptors for NDH or PGR pathways. If linear electron flow is inactive (for example in the case of DCMU addition), NADPH formation in the light is limited by chloroplast metabolism and by the stock of electrons present in PSI secondary electron donors. The optimal conditions for the poising of the photosynthetic chain to achieve maximal cyclic flow rates were largely studied *in vitro* on isolated spinach chloroplasts by Hind, Slovacek, Crowther and Mills who have shown that cyclic electron transport can be stimulated by increasing the turnover of photosystem I relative to photosystem II (using DCMU at sub-saturating concentrations) [9,10]. This stimulating effect of DCMU was suggested to prevent the over-reduction of PQs by PSII. Subsequent investigations by Hosler and Yocum confirmed this stimulating effect of DCMU on spinach thylakoid membranes, showing that the highest rates of cyclic electron flow were obtained in the complete absence of PSII activity as long as reduced ferredoxin was supplied [11].

Here, similarly to the situation obtained in intact chloroplasts treated with DCMU and sodium dithionite [8], the optimal conditions for cyclic electron flow are probably met under anoxic and DCMU conditions and justified in the following four points:

i) *Reduced ferredoxin and NADPH are accumulated*. The accumulation of reduced FDX and NADPH cannot be directly measured *in vivo*, as those two redox components have very small absorbance changes in the visible region of the spectrum. However, it can be inferred rather clearly from our study of the charge-separated state (see Results section): P_{700}–F_X^{-} is very likely formed under continuous illumination. PSI acceptors F_X and F_AF_B being reduced, thus implies that downstream carriers of higher midpoint potential (FDX and NADPH) are reduced.

ii) *Oxidized PQ are accumulated*. Similarly and for the same reasons, no direct oxidation of PQ in the light can be shown. However, like that reported in [44], we show that illumination induces a change from state 2 to state 1 (see Figs. 1 and 2), a process known to be dependent upon the oxidation of plastoquinones [64,65].

iii) *Post-illumination charge recombinations in PSI are avoided*. As can be seen in Fig. 1C and F oxidized P_{700} is not accumulated after 1 s of light, so there is no electron acceptor for F_X^{-} to recombine with. The only charge recombination that could occur is P_{700}^{+}–A_1^{-} transiently formed after a short flash superimposed to the continuous light (see Fig. 3). Therefore, in the absence of any flash, the post-illumination kinetics of Fig. 4 do not reflect charge recombination kinetics in PSI but rather the decay of membrane potential after it has been built by cyclic electron flow. In any case, charge separation–recombination processes do not contribute to the net building of a membrane potential in the light. Therefore, regardless of the cause of the destruction of the electrochromic shift in the dark, it just compensates for the building of the membrane potential in the light, which is the information relevant to us.

iv) *The steady-state membrane potential corresponds to about 3 charges per PSI*. An additional support to the productive cyclic electron flow measured under anaerobic conditions and in the presence of DCMU is given by the amplitude of the decay of the membrane potential after cessation of illumination. It is about 3 charges per PSI, a value comparable to that measured in standard conditions (aerobic without DCMU), see Fig. 4A.

4.4. Cyclic electron flow, a bifurcated pathway

The present study provides, along with a previous report [37], an estimation of the relative maximal capacities of the NDH and the PGR pathways, *in vivo*. Under mildly reducing conditions (aerobic + DCMU), cyclic flow rate is about the same in WT and *pgr5*, *i.e.* ~10–15 $e^{-}\cdot s^{-1}\cdot PSI^{-1}$, showing that the NDH pathway is preponderant over (or can substitute for) PGR under such circumstances. This conclusion is consistent with what we proposed in the first part of our work [1]. It is expected due to the more positive redox midpoint potential for NADPH (−320 mV) than for ferredoxin (−430 mV). When the reducing pressure on stromal electron carriers is mild, as is the case when PSII is inactive in aerobic conditions, electrons accumulate preferentially on $NADP^{+}$, rather than ferredoxin. The NDH pathway is therefore favored at the expense of the PGR pathway. Under more reducing conditions, as it is the case here under anaerobic conditions, cyclic electron flow rate is strongly dependent on PGR5, as shown in Fig. 4B and B′. Electrons overflow from the NDH pathway towards the PGR pathway, which appears to be of greater capacity. From our data, we can estimate that the maximum capacity of the NDH pathway is around 20 $e^{-}\cdot s^{-1}\cdot PSI^{-1}$, while that of PGR would be about 40 $e^{-}\cdot s^{-1}\cdot PSI^{-1}$, the sum of the two giving the maximum flow reported here around 60 $e^{-}\cdot s^{-1}\cdot PSI^{-1}$ (see Table 1 and Fig. 5).

Our conclusions support those of Hosler and Yocum [11] who evidenced two different pathways for cyclic electron flow, one sensitive to antimycin A, the other insensitive to the inhibitor. The former was stimulated only when NADPH relative concentration reached ≥80%,

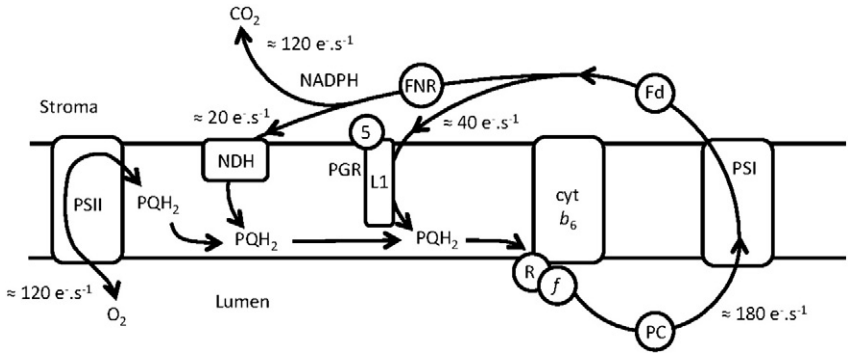

Fig. 5. Schematic drawing of the photosynthetic electron flow in *Chlamydomonas*. The figures for the maximal flow rates (in electron transferred per second per total amount of photosystems) are to be taken as estimates rather than definitive values. In this scheme, a third of the electrons transferred through PSI would be recycled. If PSI and PSII are equally abundant, a slight increase in PSI antenna size would poise the electron transfer chain under light-limiting conditions. Under saturating illumination, PQH_2 would be over-accumulated, opposing to cyclic electron flow, unless some lateral heterogeneities were expected.

i.e. ferredoxin ≥ 50% reduced, in accordance with our estimates of the anaerobic redox poise of the stroma *in vivo* ($E_h \approx -380$ mV). This early work suggested either that a threshold concentration of reduced ferredoxin was required, or a critical component became reduced at this point to activate cyclic flow [11]. The latter suggestion was recently supported by two independent studies [13,14] that showed the ferredoxin/thioredoxin system of chloroplasts regulates cyclic electron flow *in vitro*. Thioredoxin *m* interacts with PGRL1, stabilizing the monomeric, active form of the protein [14] while thioredoxin *m*4 plays a role in the down-regulation of the NDH pathway [13]. Our estimation of the redox poise of the stroma in the dark ($E_h \approx -380$ mV) and the midpoint redox potential of thioredoxin *m* ($E_{m,7} = -300$ mV) [66] suggest that anaerobic conditions would reflect a pre-activated state for the PGR pathway.

4.5. Metabolic role of cyclic electron flow

A reliable estimate of the relative contribution of cyclic electron flow to CO_2 fixation can be made with the figure of 60 $e^- \cdot s^{-1}$ as the maximal flow rate. Compared to the figure of about 120–200 electrons transferred linearly per second per photosystem, cyclic flow would contribute to about a maximum of a third to a half of the overall electron flow. The anoxic cyclic electron flow rate is significantly more than that previously reported under oxidizing conditions [1] and now matches more closely the energetic requirements calculated for carbon fixation, involving not only the Calvin cycle but also the CO_2-concentrating mechanism found in micro-algae. Here we support the conclusions of Lucker and Kramer [31].

Bendall and Manasse [5] report that under optimum conditions the average cyclic photophosphorylation rate is about 100 $\mu mol_{ATP} \cdot h^{-1} \cdot mg_{Chl}^{-1}$. Considering a coupling of 3 ATP molecules formed for each 14 protons translocated across the thylakoid membrane, and a transfer of 2 protons per electron, it gives a cyclic rate of $100/3 \times 14/2 = 233\ \mu mol_{e^-} \cdot h^{-1} \cdot mg_{Chl}^{-1}$. With the approximate equivalence (see Materials and methods) between 1 $e^- \cdot s^{-1} \cdot PSI^{-1}$ and 4 $\mu mol_{e^-} \cdot h^{-1} \cdot mg_{Chl}^{-1}$, we obtain 233/4 = 58 $e^- \cdot s^- \cdot PSI^{-1}$, in agreement with our measured rate of about 60 $e^- \cdot s^{-1} \cdot PSI^{-1}$.

4.6. Role of state transitions and cyt b_6f-PSI supercomplex formation in cyclic electron flow

State transitions modulate the relative antenna size of PSI and PSII, and because only PSI is involved in cyclic flow, they are expected to regulate, under light-limiting conditions, the relative contribution of linear and cyclic electron flows [41]. Under saturating illumination however, state transitions do not have much impact on the maximum rate of cyclic electron flow, as measured here in the presence of DCMU, see Fig. 4C and C′. Under light-limiting conditions, the effect of DCMU on cytochrome *f* oxidation level in the light is expectedly more pronounced when PSII antenna size is larger (State 1) [21–27]. We do not reject this. We disprove however, following the work of Kramer and co-workers in plants [30] and the subsequent investigations by Rappaport and co-workers [28] and Lucker and Kramer [31] in *Chlamydomonas*, that state transitions are a 'switch' between linear and cyclic electron flows.

Transition to state 2 was proposed to form cyt b_6f-PSI supercomplexes [29]. It has been disproven in the *stt7* mutant (locked in state 1), which still assembled supercomplexes when placed under anoxic conditions [28]. Recombinant PGRL1 was able to transfer electrons *in vitro* from reduced ferredoxin to plastoquinone analogues [14]. It showed that supercomplex formation is not a prerequisite for cyclic electron flow [29], although the rather slow rates obtained *in vitro* [14] do not exclude a possible role of the supercomplex in improving the catalysis. After these two recent studies [14,28], the function of the cyt b_6f-PSI supercomplex seems even more elusive. It would be highly desirable to know if *pgrl1* and *pgr5* mutants still assemble the anaerobic supercomplex or not, although if they do not it would not entirely answer the question of its functional role in cyclic electron flow. Independently from the question of the formation of a supercomplex *per se*, a co-localization of PSI, cytochrome b_6f complex and PGR in stroma lamellae would probably increase the rate of cyclic electron flow in high light. When the PQ pool becomes over-reduced around PSII in grana stacks, some catalytic amounts of oxidized PQs would remain engaged in cyclic in stroma lamellae.

The enrichment of stroma lamellae in cyt b_6f complexes upon transition to state 2 [20] does not translate into a significant increase in the maximal cyclic electron flow rate (this work and [28,31]). It rather suggests that cytochrome b_6f complex is not the limiting step for cyclic electron flow. This finding is in line with the flow rates found here and reported in Fig. 5: while cytochrome b_6f complex can sustain a linear flow of nearly 180 $e^- \cdot s^{-1}$, NDH and PGR are limited to rates below that, as shown in this work to be around 60 $e^-\ s^{-1}$.

Acknowledgements

This work would not have been possible without the contribution of Rachel Dent, Kris Niyogi and Xenie Johnson for the *pgr5* strain. Fabrice Rappaport, Giovanni Finazzi and Francis-André Wollman are warmly acknowledged for the lively and stimulating discussions that fostered these studies. I followed the footsteps of Pierre Joliot in his quest for the most appropriate experimental conditions to observe the maximal rate of cyclic electron flow, and I am grateful to him for having held my hand when tightrope walking so as not to fall in a too reduced or too oxidized plastoquinone pool. This work was supported by the Centre National de la Recherche Scientifique.

References

[1] J. Alric, J. Lavergne, F. Rappaport, Redox and ATP control of photosynthetic cyclic electron flow in *Chlamydomonas reinhardtii* (I) aerobic conditions, Biochim. Biophys. Acta 1797 (1) (2010) 44–51.
[2] D.I. Arnon, M.B. Allen, F.R. Whatley, Photosynthesis by isolated chloroplasts, Nature 174 (4426) (1954) 394–396.
[3] D.I. Arnon, R.K. Chain, Regulation of ferredoxin-catalyzed photosynthetic phosphorylations, Proc. Natl. Acad. Sci. U. S. A. 72 (12) (1975) 4961–4965.
[4] J. Alric, Cyclic electron flow around photosystem I in unicellular green algae, Photosynth. Res. 106 (1–2) (2010) 47–56.
[5] D.S. Bendall, R.S. Manasse, Cyclic photophosphorylation and electron-transport, Biochim. Biophys. Acta Bioenerg. 1229 (1) (1995) 23–38.
[6] P. Joliot, A. Joliot, Quantification of cyclic and linear flows in plants, Proc. Natl. Acad. Sci. U. S. A. 102 (13) (2005) 4913–4918.
[7] P. Joliot, J. Alric, Inhibition of CO_2 fixation by iodoacetamide stimulates cyclic electron flow and non-photochemical quenching upon far-red illumination, Photosynth. Res. 115 (1) (2013) 55–63.
[8] D. Crowther, G. Hind, Partial characterization of cyclic electron transport in intact chloroplasts, Arch. Biochem. Biophys. 204 (2) (1980) 568–577.
[9] J.D. Mills, R.E. Slovacek, G. Hind, Cyclic electron transport in isolated intact chloroplasts. Further studies with antimycin, Biochim. Biophys. Acta 504 (2) (1978) 298–309.
[10] R.E. Slovacek, D. Crowther, G. Hind, Relative activities of linear and cyclic electron flows during chloroplast CO_2-fixation, Biochim. Biophys. Acta 592 (3) (1980) 495–505.
[11] J.P. Hosler, C.F. Yocum, Regulation of cyclic photophosphorylation during ferredoxin-mediated electron transport: effect of DCMU and the NADPH/NADP ratio, Plant Physiol. 83 (4) (1987) 965–969.
[12] J.F. Allen, Cyclic, pseudocyclic and noncyclic photophosphorylation: new links in the chain, Trends Plant Sci. 8 (1) (2003) 15–19.
[13] A. Courteille, et al., Thioredoxin m4 controls photosynthetic alternative electron pathways in *Arabidopsis*, Plant Physiol. 161 (1) (2013) 508–520.
[14] A.P. Hertle, et al., PGRL1 is the elusive ferredoxin-plastoquinone reductase in photosynthetic cyclic electron flow, Mol. Cell 49 (3) (2013) 511–523.
[15] P.V. Sane, Dj Goodchil, R.B. Park, Characterization of chloroplast photosystems-1 and photosystems-2 separated by a non-detergent method, Biochim. Biophys. Acta 216 (1) (1970) 168–178.
[16] B. Andersson, J.M. Anderson, Lateral heterogeneity in the distribution of chlorophyll–protein complexes of the thylakoid membranes of spinach chloroplasts, Biochim. Biophys. Acta 593 (2) (1980) 427–440.
[17] R.P. Cox, B. Andersson, Lateral and transverse organisation of cytochromes in the chloroplast thylakoid membrane, Biochem. Biophys. Res. Commun. 103 (4) (1981) 1336–1342.
[18] J.M. Anderson, Distribution of the cytochromes of spinach chloroplasts between the appressed membranes of grana stacks and stroma-exposed thylakoid regions, FEBS Lett. 138 (1) (1982) 62–66.
[19] F.A. Wollman, State transitions reveal the dynamics and flexibility of the photosynthetic apparatus, EMBO J. 20 (14) (2001) 3623–3630.
[20] O. Vallon, et al., Lateral redistribution of cytochrome b6/f complexes along thylakoid membranes upon state transitions, Proc. Natl. Acad. Sci. U. S. A. 88 (18) (1991) 8262–8266.
[21] G. Forti, et al., In vivo changes of the oxidation–reduction state of NADP and of the ATP/ADP cellular ratio linked to the photosynthetic activity in *Chlamydomonas reinhardtii*, Plant Physiol. 132 (3) (2003) 1464–1474.
[22] G. Finazzi, et al., Involvement of state transitions in the switch between linear and cyclic electron flow in *Chlamydomonas reinhardtii*, EMBO Rep. 3 (3) (2002) 280–285.
[23] G. Finazzi, et al., Nonphotochemical quenching of chlorophyll fluorescence in *Chlamydomonas reinhardtii*, Biochemistry 45 (5) (2006) 1490–1498.
[24] G. Finazzi, et al., State transitions, cyclic and linear electron transport and photophosphorylation in *Chlamydomonas reinhardtii*, Biochim. Biophys. Acta 1413 (3) (1999) 117–129.
[25] G. Finazzi, G. Forti, Metabolic flexibility of the green alga *Chlamydomonas reinhardtii* as revealed by the link between state transitions and cyclic electron flow, Photosynth. Res. 82 (3) (2004) 327–338.
[26] G. Finazzi, et al., Photoinhibition of *Chlamydomonas reinhardtii* in state 1 and state 2: damages to the photosynthetic apparatus under linear and cyclic electron flow, J. Biol. Chem. 276 (25) (2001) 22251–22257.
[27] G. Finazzi, The central role of the green alga *Chlamydomonas reinhardtii* in revealing the mechanism of state transitions, J. Exp. Bot. 56 (411) (2005) 383–388.
[28] H. Takahashi, et al., Cyclic electron flow is redox-controlled but independent of state transition, Nat. Commun. 4 (2013) 1954.
[29] M. Iwai, et al., Isolation of the elusive supercomplex that drives cyclic electron flow in photosynthesis, Nature 464 (7292) (2010) 1210–1213.
[30] D. Strand, A. Livingston, D. Kramer, Do state transitions control CEF1 in higher plants? Photosynthesis Research for Food, Fuel and the Future, Springer, Berlin/Heidelberg, 2013, pp. 286–289.
[31] B. Lucker, D.M. Kramer, Regulation of cyclic electron flow in *Chlamydomonas reinhardtii* under fluctuating carbon availability, Photosynth. Res. 117 (1–3) (2013) 449–459.
[32] P. Joliot, A. Joliot, Cyclic electron flow in C3 plants, Biochim. Biophys. Acta 1757 (5–6) (2006) 362–368.
[33] X. Johnson, J. Alric, Interaction between starch breakdown, acetate assimilation, and photosynthetic cyclic electron flow in *Chlamydomonas reinhardtii*, J. Biol. Chem. 287 (31) (2012) 26445–26452.
[34] X. Johnson, J. Alric, Central carbon metabolism and electron transport in *Chlamydomonas reinhardtii*: metabolic constraints for carbon partitioning between oil and starch, Eukaryot. Cell 12 (6) (2013) 776–793.
[35] L. Houille-Vernes, et al., Plastid terminal oxidase 2 (PTOX2) is the major oxidase involved in chlororespiration in *Chlamydomonas*, Proc. Natl. Acad. Sci. U. S. A. 108 (51) (2011) 20820–20825.
[36] F. Jans, et al., A type II NAD(P)H dehydrogenase mediates light-independent plastoquinone reduction in the chloroplast of *Chlamydomonas*, Proc. Natl. Acad. Sci. U. S. A. 105 (51) (2008) 20546–20551.
[37] D. Tolleter, et al., Control of hydrogen photoproduction by the proton gradient generated by cyclic electron flow in *Chlamydomonas reinhardtii*, Plant Cell 23 (7) (2011) 2619–2630.
[38] D.A. Moss, D.S. Bendall, Cyclic electron-transport in chloroplasts — the Q-cycle and the site of action of antimycin, Biochim. Biophys. Acta 767 (3) (1984) 389–395.
[39] X. Johnson, et al., PGR5-mediated Cyclic Electron Flow under ATP- or Redox-limiting Conditions, a Study of Pgr5 ΔATPase and Pgr5 ΔrbcL Mutants in *Chlamydomonas reinhardtii*, Plant Physiol. (2014) (accepted in revised form).
[40] D. Leister, T. Shikanai, Complexities and protein complexes in the antimycin A-sensitive pathway of cyclic electron flow in plants, Front. Plant Sci. 4 (2013) 161.
[41] P. Cardol, et al., Impaired respiration discloses the physiological significance of state transitions in *Chlamydomonas*, Proc. Natl. Acad. Sci. U. S. A. 106 (37) (2009) 15979–15984.
[42] N. Depege, S. Bellafiore, J.D. Rochaix, Role of chloroplast protein kinase Stt7 in LHCII phosphorylation and state transition in *Chlamydomonas*, Science 299 (5612) (2003) 1572–1575.
[43] G. Peers, et al., An ancient light-harvesting protein is critical for the regulation of algal photosynthesis, Nature 462 (7272) (2009) 518–521.
[44] P. Delepelaire, F.A. Wollman, Correlations between fluorescence and phosphorylation changes in thylakoid membranes of *Chlamydomonas reinhardtii* in vivo: a kinetic analysis, Biochim. Biophys. Acta Bioenerg. 809 (2) (1985) 277–283.
[45] F.A. Wollman, P. Delepelaire, Correlation between changes in light energy distribution and changes in thylakoid membrane polypeptide phosphorylation in *Chlamydomonas reinhardtii*, J. Cell Biol. 98 (1) (1984) 1–7.
[46] I.D. Kuntz, M. Calvin, Kinetic studies of the two light reactions in photosynthesis, Photochem. Photobiol. 4 (3) (1965) 537–548.
[47] K. Takizawa, et al., The thylakoid proton motive force in vivo. Quantitative, non-invasive probes, energetics, and regulatory consequences of light-induced pmf, Biochim. Biophys. Acta 1767 (10) (2007) 1233–1244.
[48] C.A. Sacksteder, D.M. Kramer, Dark-interval relaxation kinetics (DIRK) of absorbance changes as a quantitative probe of steady-state electron transfer, Photosynth. Res. 66 (1–2) (2000) 145–158.
[49] C.A. Sacksteder, et al., The proton to electron stoichiometry of steady-state photosynthesis in living plants: a proton-pumping Q cycle is continuously engaged, Proc. Natl. Acad. Sci. U. S. A. 97 (26) (2000) 14283–14288.
[50] P. Joliot, A. Joliot, Cyclic electron transfer in plant leaf, Proc. Natl. Acad. Sci. U. S. A. 99 (15) (2002) 10209–10214.
[51] J.A. Cruz, et al., Contribution of electric field (Delta psi) to steady-state transthylakoid proton motive force (pmf) in vitro and in vivo. Control of pmf parsing into Delta psi and Delta pH by ionic strength, Biochemistry 40 (5) (2001) 1226–1237.
[52] T.J. Avenson, J.A. Cruz, D.M. Kramer, Modulation of energy-dependent quenching of excitons in antennae of higher plants, Proc. Natl. Acad. Sci. U. S. A. 101 (15) (2004) 5530–5535.
[53] C. Klughammer, K. Siebke, U. Schreiber, Continuous ECS-indicated recording of the proton-motive charge flux in leaves, Photosynth. Res. 117 (1–3) (2013) 471–487.
[54] D.I. Arnon, Copper enzymes in isolated chloroplasts. Polyphenoloxidase in *Beta vulgaris*, Plant Physiol. 24 (1) (1949) 1–15.
[55] P.J. Neale, A. Melis, Algal photosynthetic membrane complexes and the photosynthesis-irradiance curve: a comparison of light-adaptation responses in *Chlamydomonas reinhardtii* (CHLOROPHYTA)1, J. Phycol. 22 (4) (1986) 531–538.
[56] P. Joliot, R. Delosme, Flash-induced 519 nm absorption change in green algae, Biochim. Biophys. Acta Bioenerg. 357 (2) (1974) 267–284.
[57] Y.V. Bolychevtseva, et al., Effects of oxygen and photosynthesis carbon cycle reactions on kinetics of P700 redox transients in cyanobacterium *Arthrospira platensis* cells, Biochemistry (Mosc) 72 (3) (2007) 275–281.
[58] B. Ghysels, et al., Function of the chloroplast hydrogenase in the microalga *Chlamydomonas*: the role of hydrogenase and state transitions during photosynthetic activation in anaerobiosis, PLoS One 8 (5) (2013) e64161.
[59] L. Bulté, et al., ATP control on state transitions in vivo in *Chlamydomonas reinhardtii*, Biochim. Biophys. Acta Bioenerg. 1020 (1) (1990) 72–80.
[60] G. Peltier, P. Thibault, O(2) uptake in the light in *Chlamydomonas*: evidence for persistent mitochondrial respiration, Plant Physiol. 79 (1) (1985) 225–230.
[61] D.F. Sueltemeyer, K. Klug, H.P. Fock, Effect of photon fluence rate on oxygen evolution and uptake by *Chlamydomonas reinhardtii* suspensions grown in ambient and CO(2)-enriched air, Plant Physiol. 81 (2) (1986) 372–375.
[62] P.C. Maxwell, J. Biggins, Role of cyclic electron-transport in photosynthesis as measured by photoinduced turnover of P-700 in vivo, Biochemistry 15 (18) (1976) 3975–3981.
[63] K. Brettel, W. Leibl, Electron transfer in photosystem I, Biochim. Biophys. Acta 1507 (1–3) (2001) 100–114.
[64] P. Horton, et al., Regulation of phosphorylation of chloroplast membrane polypeptides by the redox state of plastoquinone, FEBS Lett. 125 (2) (1981) 193–196.
[65] J.F. Allen, et al., Chloroplast protein phosphorylation couples plastoquinone redox state to distribution of excitation energy between photosystems, Nature 291 (1981) 25–29.
[66] M. Hirasawa, et al., Oxidation–reduction properties of chloroplast thioredoxins, ferredoxin:thioredoxin reductase, and thioredoxin f-regulated enzymes, Biochemistry 38 (16) (1999) 5200–5205.